










## RESEARCH ARTICLE OPEN ACCESS

# Variation in Cell Wall Composition and Saccharification Potential of Seed-Based *Miscanthus* Hybrids Grown on Marginal Lands Across Six European Trial Locations

Kasper van der Cruijssen<sup>1</sup> | Mohamad Al Hassan<sup>1</sup>  | Oene Dolstra<sup>1</sup> | Elena Magenau<sup>2</sup>  | Mislav Kontek<sup>3</sup> | Chris Ashman<sup>4</sup>  | Danny Awty-Carroll<sup>4,5</sup>  | Andrea Ferrarini<sup>6</sup>  | Enrico Martani<sup>6,7</sup>  | Phillip van der Pluijm<sup>8</sup> | Gert-Jan Petri<sup>9</sup> | Emmanuel de Maupéou<sup>8</sup> | Maria-João Paulo<sup>10</sup> | Jason Kam<sup>11</sup> | Bert-Jan van Dinter<sup>12</sup> | Lars Kraak<sup>12</sup> | Annemarie Dechesne<sup>1</sup> | Vanja Jurišić<sup>3</sup> | Iris Lewandowski<sup>2</sup> | Stefano Amaducci<sup>8</sup> | John Clifton-Brown<sup>4,13</sup>  | Andreas Kiesel<sup>2</sup>  | Luisa M. Trindade<sup>1</sup> 

<sup>1</sup>Laboratory of Plant Breeding, Wageningen University and Research, Wageningen, the Netherlands | <sup>2</sup>Institute of Crop Science, University of Hohenheim, Stuttgart, Germany | <sup>3</sup>Faculty of Agriculture, University of Zagreb, Zagreb, Croatia | <sup>4</sup>Institute of Biological, Environmental and Rural Sciences, Aberystwyth University, Aberystwyth, UK | <sup>5</sup>School of Biological and Environmental Sciences, Liverpool John Moores University, Liverpool, UK | <sup>6</sup>Department of Sustainable Crop Production, Università Cattolica del Sacro Cuore, Piacenza, Italy | <sup>7</sup>Davines Group—Rodale Institute European Regenerative Organic Center (ERO), Parma, Italy | <sup>8</sup>Novabiom, Ferme de Vauventriers, Champhol, France | <sup>9</sup>Miscanthusgroep, Zwanenburg, the Netherlands | <sup>10</sup>Biometris, Wageningen University and Research, Wageningen, the Netherlands | <sup>11</sup>Terravesta Ltd., Lincoln, UK | <sup>12</sup>Vandinter Semo, Scheemda, the Netherlands | <sup>13</sup>Department of Agronomy and Plant Breeding, Research Centre for Biosystems, Land-Use and Nutrition (IFZ), Justus Liebig University, Gießen, Germany

**Correspondence:** Luisa M. Trindade ([luisa.trindade@wur.nl](mailto:luisa.trindade@wur.nl))

**Received:** 18 March 2025 | **Accepted:** 3 June 2025

**Funding:** This project has received funding from the Bio-based Industries Joint Undertaking under the European Union's Horizon 2020 research and innovation program under grant agreement No 745012 (GRACE).

**Keywords:** biomass quality | cell wall composition | intraspecific and interspecific hybrids | lignocellulosic biofuel | miscanthus | saccharification efficiency

## ABSTRACT

*Miscanthus* breeding programs have focused on developing intraspecific (*M. sinensis* × *M. sinensis*) and interspecific (*M. sinensis* × *M. sacchariflorus*) seed-based hybrids with distinct cell wall characteristics for different biomass value chains. Here, we evaluated the performance of 13 novel hybrids (including seed-based intraspecific, seed-based interspecific, and one clonally propagated interspecific hybrid) relative to *Miscanthus* × *giganteus* (*M* × *g*). We compared the cell wall composition, saccharification efficiency, and yield after spring harvests in 2021 and 2022 across six European locations. Cell wall content and composition varied significantly among hybrids and were influenced by environmental conditions, yet differences due to parental background were largely consistent across locations. On average, seed-based interspecific hybrids (80.6%–84.0% neutral detergent fiber) had a lower total cell wall content than the other hybrids evaluated in this study (88.3%–90.8%). In contrast, cellulose was ~5.5% higher in hybrids with an *M. sinensis* × *M. sacchariflorus* background relative to the intraspecific hybrids, while hemicellulose averaged above 34% for intraspecific hybrids, 29.4% to 31.8% in the interspecific hybrids, and below 27% for *M* × *g*. Lignin content was highest in *M* × *g* (~13.8%), intermediate in the interspecific hybrids (11.0%–12.2%), and lowest in the intraspecific hybrids (~10%). These compositional traits translated into saccharification efficiencies that were 32.9% higher for the intraspecific hybrids and 9.8%–13.1% higher for the interspecific hybrids (seed-based and clonally propagated) compared to *M* × *g*. Accounting for biomass yield, either several seed-based hybrids or the novel clonally propagated hybrid exceeded the theoretical ethanol potential of *M* × *g* at all trial locations, indicating strong potential for their use in lignocellulosic biofuel production.

This is an open access article under the terms of the [Creative Commons Attribution](https://creativecommons.org/licenses/by/4.0/) License, which permits use, distribution and reproduction in any medium, provided the original work is properly cited.

© 2025 The Author(s). *GCB Bioenergy* published by John Wiley & Sons Ltd.

## 1 | Introduction

Miscanthus is a genus of rhizomatous grass species containing promising candidate crops for the production of lignocellulosic biomass on marginal lands. The main advantages of miscanthus are its efficient use of resources, such as nutrients, water, and light, and resilience towards harsh and unfavorable conditions (van der Weijde et al. 2013). In particular, *M. × giganteus* (*M×g*) is renowned for its exceptional yields, ranging from 9 to 15 Mg ha<sup>-1</sup> when cultivated on marginal lands in Europe (Amaducci et al. 2017; Jeżowski et al. 2017). Although *M×g* has many favorable traits, its cultivation and utilization are not without limitations. First, *M×g* is a sterile hybrid originating from a wild crossing between *M. sacchariflorus* (*M. sac*) × *M. sinensis* (*M. sin*) that is multiplied through rhizome propagation. The low multiplication rate of rhizome-based propagation methods limits the possibilities for rapid expansion of the cultivation area, while it also contributes to high establishment costs per hectare (Xue et al. 2015; Clifton-Brown et al. 2017). Additionally, previous research showed that the potential of miscanthus exceeds that of *M×g*, as evidenced by the identification of higher yielding accessions and those with a more desirable feedstock composition (van der Weijde, Kiesel, et al. 2017; Clark et al. 2019). Utilizing the natural variation present in *M. sac* and *M. sin* allows for further breeding of genetically improved varieties, in contrast to the legacy *M×g* cultivars, which lack genetic variation as they were all derived from the same sterile clone (Głowacka et al. 2015).

Breeding seed-based miscanthus hybrids offers a solution to the limitations of rhizome-based propagation, while simultaneously enabling the genetic optimization of cell wall composition to improve suitability for bioconversion (Clifton-Brown et al. 2017; van der Crujisen et al. 2021). Cell walls provide strength and protection to plants, achieved by the formation of a thick secondary cell wall layer during plant development (Zhang et al. 2021). Lignin is incorporated into the cell wall matrix during this process, where along with cellulose and hemicellulose it forms a complex and rigid structure (van der Weijde, Dolstra, et al. 2017; Zhong et al. 2019). Considering that cell walls make up 80%–90% of miscanthus biomass at harvest, their exact composition is a critical factor determining the biomass's suitability for bioconversion. For instance, the production of bioethanol requires the enzymatic breakdown of cellulose into glucose monomers. This process is impeded by lignin, which forms a physical barrier to which these enzymes adhere (Taherzadeh and Karimi 2008; Li, Liao, et al. 2016). Utilization of specific components therefore requires decoupling the different cell wall polymers from a matrix that is naturally resistant to degradation. Although severe pretreatments can break up the cell wall matrix, they lead to the formation of inhibitory components that limit both saccharification efficiency and the fermentation of sugars into ethanol (Cunha et al. 2019; Zhai et al. 2022). Additionally, severe pretreatments put a constraint on sustainability and add considerable costs to the bioconversion process (Limayem and Ricke 2012; Boakye-Boaten et al. 2017). Accessions featuring more favorable cell wall compositions would be advantageous, as they could make the biomass more receptive

to pretreatments and potentially reduce pretreatment severity (van der Crujisen et al. 2021).

Although the cell wall composition is largely genetically determined (Sheng et al. 2017; van der Weijde, Kamei, et al. 2017; Zeng, Sheng, Zhu, Wei, et al. 2020; Zeng, Sheng, Zhu, Zhao, et al. 2020), it is also affected by the environmental conditions plants are exposed to during the growing season. Many of such changes have been associated with abiotic stress factors that force the plant to adapt many critical processes, including their cell wall biosynthesis (Gall et al. 2015). Research on miscanthus has shown that several abiotic stresses significantly affect the cell wall composition, generally increasing the conversion efficiency from cellulose to glucose (van der Weijde, Huxley, et al. 2017; Cheng et al. 2018; da Costa et al. 2018; Hoover et al. 2018; van der Crujisen et al. 2024). The prospect of cultivating miscanthus mainly on marginal and degraded lands means that plants will likely have to endure unfavorable conditions leading to abiotic stress(es) at some point during the growing season (Quinn et al. 2015). Therefore, it is important to extensively evaluate the performance and stability of newly developed miscanthus hybrids grown under marginal conditions.

In recent years, several promising intra- (*M. sin* × *M. sin*) and interspecific (*M. sac* × *M. sin*) seed-based miscanthus hybrids have been developed at the Laboratory of Plant Breeding at Wageningen University and Research (WUR) and the Institute of Biological, Environmental and Rural Sciences (IBERS) at Aberystwyth University, respectively. The objective of this research was to assess the potential of these seed-based intra- and interspecific hybrids in terms of biomass quality and quantity when cultivated on marginal lands across Europe. In order to do this, trials containing 14 miscanthus hybrids were established under various marginal conditions in six European countries. Plants were harvested in two consecutive growth years and analyzed for the major cell wall components and their cellulose conversion efficiency. The results showed that the difference in environmental conditions between trial environments and the fluctuation between growth years affected the cell wall composition in both intra- and interspecific hybrids. Also, it could be concluded that, depending on local conditions, seed-based hybrids are a viable alternative to *M×g*.

## 2 | Materials and Methods

### 2.1 | Plant Material and Trial Setup

Thirteen novel miscanthus hybrids and *M×g* (GRC 9) were grown in six multilocation trials across marginal lands in Europe. Eight of these (GRC 1–8) were seed-based intraspecific (*M. sin* × *M. sin*) hybrids that were selected from the breeding program at Wageningen University. Four interspecific (*M. sac* × *M. sin*) seed-based hybrids (GRC 10–11 and GRC 13–14) were selected from the IBERS breeding program. Lastly, a clonally propagated interspecific hybrid (GRC 15), which was supplied by Terravesta Ltd. (Lincoln, United Kingdom) and included in the trials (Table 1). The trials were located on marginal lands

**TABLE 1** | Plant species, propagation method and planting density of the 14 miscanthus hybrids used in this study.

ID	Plant species	Propagation	Plant density (m <sup>-2</sup> )
GRC 1–8	<i>M. sinensis</i> × <i>M. sinensis</i>	Seed	3
GRC 9	<i>M. × giganteus</i>	Rhizome	1.5
GRC 10–11, 13–14	<i>M. sacchariflorus</i> × <i>M. sinensis</i>	Seed	1.5
GRC 15	<i>M. sacchariflorus</i> × <i>M. sinensis</i>	Rhizome	1.5

across six different countries: Croatia (Zagreb, ZAG), France (Chanteloup-les-Vignes, CHV), Germany (Oberer Lindenhof, OLI), Italy (Piacenza, PAC), The Netherlands (Schiphol, SCH) and Wales (Trawsgoed, TWS). Each trial location exhibited unique characteristics and reasons for marginality (Figure 1); further details of these trials have been described by Awty-Carroll et al. (2022).

Seeds of the seed-based hybrids were germinated in plugs and grown into 2–3-month-old plantlets inside of the greenhouse. In 2018, these plugs and rhizomes were planted in 96 m<sup>2</sup> plots that had a density of either 3 plants m<sup>-2</sup> (*M. sin* × *M. sin*) or 1.5 plants m<sup>-2</sup> (*M. sac* × *M. sin* and *M. × giganteus*). The plots were established according to a randomized complete block design with four replicates per hybrid, leading to a total of 56 plots per trial location. From each plot, five consecutively growing plants were selected for individual harvest and used for further measurements.

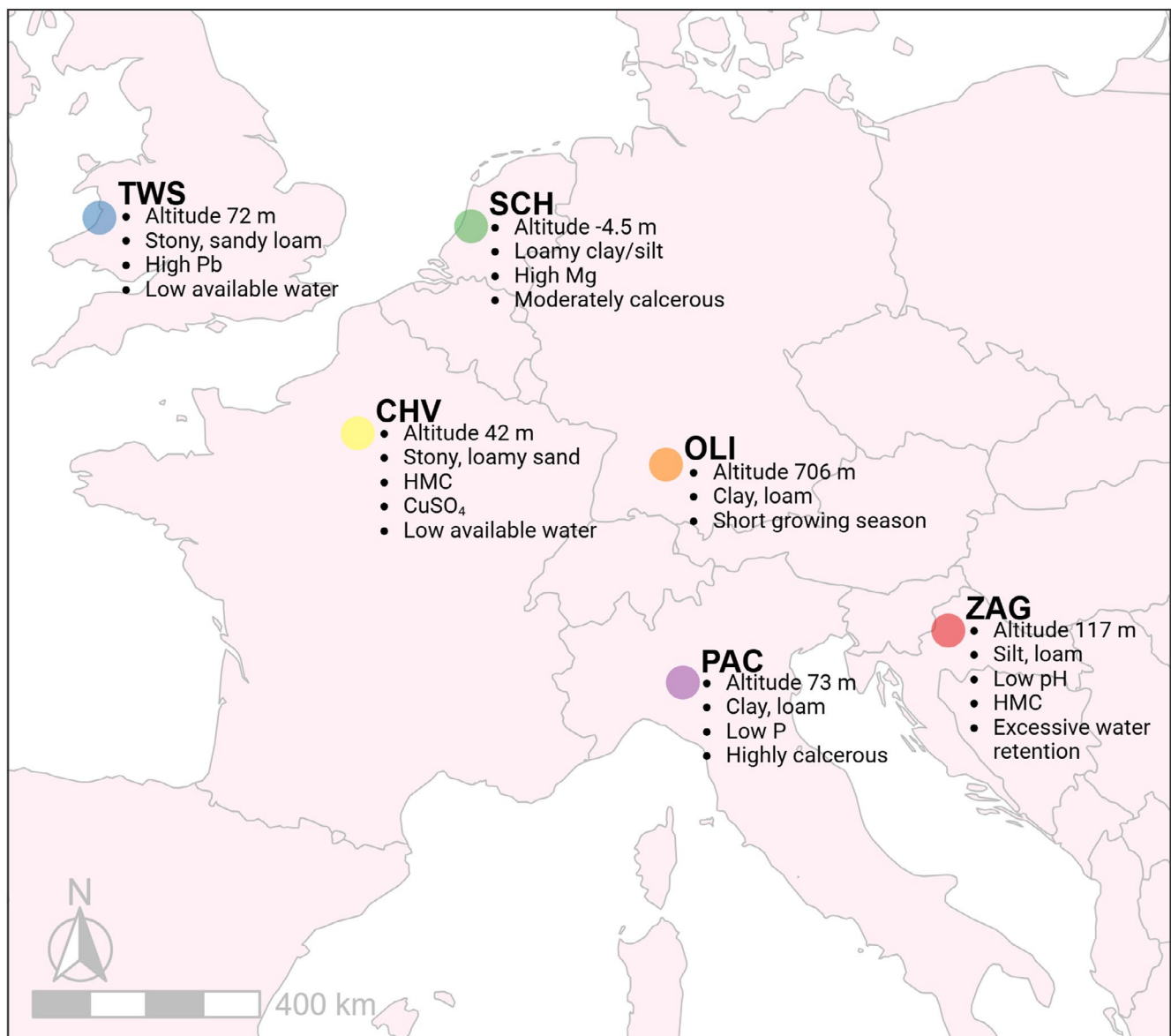


**FIGURE 1** | Trial locations and conditions. CHV = Chanteloup-les-Vignes, CuSO<sub>4</sub> = copper sulfate, HMC = heavy metal contaminated, Mg = magnesium, OLI = Oberer Lindenhof, P = phosphorus, PAC = Piacenza, Pb = lead, SCH = Schiphol, TWS = Trawsgoed, ZAG = Zagreb.

## 2.2 | Yield Measurements and Biomass Preparation

Plant harvests took place between February and March at the different trial locations in 2021 and 2022. In 2021, the fresh weight of the five individually harvested plants per plot was determined 2 days after harvesting to avoid variations caused by surface moisture. This was done for four replicate plots, with five plants per plot, resulting in a total of 20 plants from each hybrid at each location. Each plant was separated into stem and leaf fractions that were weighed separately. A representative subsample of several stems per plant was oven-dried to a constant weight at 60°C and used to calculate the dry weight of each plant. Unfortunately, direct planted  $M \times g$  rhizomes had extremely poor establishment at the sites CHV and SCH, making (reliable) yield assessments impossible. In order to provide a yield estimation at SCH, plants from  $M \times g$  were retrieved from a larger field scale trial that was also planted in 2018 and located adjacently to the studied plots. The dried stems were chipped into ~2 cm pieces and were milled on a cross-beater mill equipped with a 1 mm sieve. The milled stem samples were used for further laboratory analysis.

## 2.3 | NIRS Prediction of Cell Wall Composition and Saccharification Efficiency

Near-infrared spectroscopy (NIRS) prediction models were established for the high-throughput assessment of neutral detergent fiber (NDF), acid detergent fiber (ADF), acid detergent lignin (ADL) and cellulose conversion of stem samples, similarly as described by van der Weijde, Dolstra, et al. (2017), van der Weijde, Huxley, et al. (2017), van der Weijde, Kamei, et al. (2017), van der Weijde, Kiesel, et al. (2017). In brief, all stem samples were milled into 1 mm particles on a cross-beater mill and scanned on a near-infrared spectrometer (Foss DS2500, Foss, Hillerød, Denmark) to obtain the spectral data from 400 to 2500 nm at 0.5 nm intervals. The spectra were preprocessed in WinISI 4.9 (Foss, Hillerød, Denmark) using the Standard Normal Variate (SNV) transformation and were subsequently detrended, while parameters for derivative calculation were set at 1-12-12-1. In here, the first number indicates the derivative number, the second number indicates the gap over which derivation is applied, and the last two numbers indicate the datapoints used for smoothing. From the spectra, 200 samples were selected for construction of prediction models for NDF, ADF, and ADL, while 100 samples were selected for construction of a prediction model for cellulose conversion. The selected samples were analyzed biochemically (described below) and the data were aligned to the spectra within the software to construct the NIRS prediction models. External validation samples were randomly selected (35 for cell wall composition, 25 for saccharification efficiency) for validation of the prediction models. The internal calibration set and external validation set showed a high level of predictability for NDF, ADF, ADL, and cellulose conversion (Table S1). The cell wall components cellulose (ADF-ADL), hemicellulose (NDF-ADF) and (acid detergent) lignin

(ADL) were calculated from the NIRS predicted values for NDF, ADF and ADL.

## 2.4 | Cell Wall Compositional Analysis

The selected samples for the construction and validation of the prediction model were analyzed for neutral detergent fiber (NDF), acid detergent fiber (ADF), and acid detergent lignin (ADL) according to the principles established by Van Soest et al. (1991). The procedures for NDF and ADF were performed using an ANKOM 2000 Automated Fiber Analyzer (ANKOM Technology, Macedon, NY, United States), following the analytical procedures provided by the manufacturer. ADF residues were submerged in 72% (w/w)  $H_2SO_4$  for 3 h according to the protocol, after which ADL was obtained as the solid fraction. All analyses were performed in duplicate.

## 2.5 | Saccharification Efficiency

The analytical procedure for saccharification efficiency was essentially performed as described by van der Weijde et al. (2016). Stem samples (~500 mg) were treated with  $\alpha$ -amylase and washed with deionized water (3 $\times$ , 50°C, 5 min) to remove starch and soluble sugars. Pretreatment was performed with 2% (w/w) NaOH (160 RPM, 50°C, 2 h) in an incubator shaker (Innova 42, New Brunswick Scientific, Edison, NJ, United States). Pretreated samples were subsequently washed for 5 min with deionized water (2 $\times$ ) and 0.1 M sodium citrate buffer (pH 5.0) at 50°C, 160 RPM. Stem samples were dissolved in sodium citrate buffer (pH 5.0), with 0.02% (v/v) Proclin (Sigma-Aldrich, St Louis, MO, United States) added to prevent microbial growth (He et al. 2019). An excess of cellulase enzyme blend (SAE0020, Sigma-Aldrich, St Louis, MO, United States) was added to each sample (30% (w/w) g enzyme/g cellulose) to ensure maximum saccharification levels were achieved within the incubation period under constant shaking (160 RPM, 50°C, 48 h). The amount of glucose that was released from each sample was quantified with a high performance anion exchange chromatograph (Dionex ICS 5000+ DC, Thermo Fisher Scientific, Waltham, MA, United States) equipped with a Dionex CarboPac PA-1 column and corrected for the initial sample weight. The amount of glucose released was used to calculate the percentage of the total cellulose content that was converted into glucose. In turn, the cellulose conversion (%) was used to calculate the theoretical ethanol yields, also taking into account biomass yield and composition. The following formulas were adapted from van der Weijde, Dolstra, et al. (2017), van der Weijde, Huxley, et al. (2017), van der Weijde, Kamei, et al. (2017), van der Weijde, Kiesel, et al. (2017):

$$\text{Cellulose conversion \%} = \frac{\text{Glucose release (\% DM)}}{\text{Cellulose (\% DM)} \times 1.111} \times 100$$

1.111 accounts for the molecular weight difference between cellulose and glucose as water molecules are removed during the polymerization process

$$\text{Theoretical ethanol yield (g m}^{-2}\text{)} = \frac{\text{Yield (g m}^{-2}\text{)} \times \text{Cellulose} \times \text{Cellulose conversion} \times 2 \times \text{MwE}}{\text{MwG}}$$

MwE is the molecular weight of ethanol (46.07 g/mol) and MwG is the molecular weight of glucose (180.16 g/mol). The number 2 refers to the ethanol molecules formed per glucose molecule. The calculation for theoretical ethanol yield assumes full conversion of available cellulose into ethanol.

## 2.6 | Statistical Analysis

All statistical analyses were performed in R (R-4.5.0, Lenth 2025). For all of the NIRS predicted traits (cellulose, hemicellulose, lignin and cellulose conversion) analyses of variance (ANOVAs) were performed on plot averages using linear mixed models, which were specified using lme4 (Bates et al. 2015) and analyzed using lmerTest v3.1-3 (Kuznetsova et al. 2017). Here,  $Y_{ijk}$  represents the response variable,  $\mu$  is the grand mean,  $H_i$  is the fixed effect of hybrid,  $L_j$  is the fixed effect of trial location,  $Y_k$  is the fixed year effect,  $B_r(L_j Y_k)$  is the random block effect,  $HL_{ij}$  is the interaction term between hybrid and location,  $HY_{ik}$  is the interaction term between hybrid and year,  $LY_{jk}$  is the interaction term between location and year,  $HL_{ijk}$  is the interaction term between hybrid, location, year, and  $\varepsilon_{ijk}$  is the residual error:

$$Y_{ijk} = \mu + H_i + L_j + Y_k + B_r(L_j Y_k) + HL_{ij} + HY_{ik} + LY_{jk} + HLY_{ijk} + \varepsilon_{ijk}$$

Similarly, for yield measurements, ANOVA was performed on plot averages using a linear mixed model where  $Y_{ijk}$  represents the response variable,  $\mu$  is the grand mean,  $H_i$  is the fixed effect of hybrid,  $L_j$  is the fixed effect of trial location,  $B_k(L_j)$  is the random block effect,  $HL_{ij}$  is the interaction term between hybrid and location, and  $\varepsilon_{ijk}$  is the residual error:

$$Y_{ijk} = \mu + H_i + L_j + B_k(L_j) + HL_{ij} + \varepsilon_{ijk}$$

The emmeans package (Lenth 2023) was utilized to estimate marginal means and conduct Tukey's post hoc tests across hybrids. For stem yield, the post hoc test was performed per trial location, while for cell wall-related traits, the analysis was performed across locations but separately for each year. Pearson correlations between traits were performed on plot averages across all trial locations and included both years. Figures were created using the ggplot2 package (Wickham 2016).

## 3 | Results and Discussion

### 3.1 | Cell Wall Composition Differs Significantly Between Intra- and Interspecific Hybrids

In two consecutive years, eight intraspecific (GRC 1–8) and four interspecific (GRC 10–11/13–14) seed-based miscanthus hybrids,  $M \times g$  (GRC9) and another rhizome-propagated  $M. sac \times M. sin$  (GRC15) were evaluated for cell wall content and composition when grown on marginal lands. According to the statistical test results, hybrids explained a significant and substantial part of the variation found in cell wall content and composition (Tables S2 and S3). Averaged across trials and years, the cell wall content (NDF) of the dried stems ranged between 80% and 91%, which is similar to previously reported values for miscanthus

(Allison et al. 2011; van der Weijde, Dolstra, et al. 2017). The results showed that at every trial location, the hybrids could be divided into two distinct groups based on their cell wall content. On the one hand, GRC 1–8, GRC 9, and GRC 15, of which the average cell wall content ranged between 88.3% and 90.8%. On the other hand, GRC 10–11 and GRC 13–14, of which the average cell wall content ranged between 80.6% and 84.0%. Although there were small degrees of variation within both groups, it stood out that at all trial locations, the values of seed-based  $M. sac \times M. sin$  hybrids were consistently lower compared to the other hybrids (Figure 2a). The contrast with the interspecific clonally propagated genotypes implies that lower values were related specifically to this particular set of seed-based  $M. sac \times M. sin$  hybrids. Previous work agrees with this premise, as cell wall content had equal distributions among  $M. sacchariflorus$  and  $M. sinensis$  accessions (Allison et al. 2011). As indicated by Awty-Carroll et al. (2022) and Magenau et al. (2022), the seed-based  $M. sac \times M. sin$  hybrids had a longer growth period and matured later than the other hybrids that were studied in these trials. The cell wall content in grasses accumulates gradually during development, initially due to the increase of cellulose and hemicellulose and eventually lignification leads to cell wall thickening (Jung and Casler 2006; Rancour et al. 2012; Matos et al. 2013). As a consequence, the upper internodes of the stems have less developed cell walls (Sarath et al. 2007; Hu et al. 2017). Therefore, the lower cell wall content in seed-based  $M. sac \times M. sin$  hybrids might have originated partly from the younger upper parts of the stems that developed later in the growing season. Additionally, the general lack of senescence in these hybrids likely results in higher proportions of non-structural cell components remaining, such as proteins, soluble sugars, and minerals (Godin et al. 2013; Jensen et al. 2017). This also contributes to the lower cell wall content retrieved per gram of dry matter. Since cell walls are the harvestable product from lignocellulosic crops, the lower cell wall content of these hybrids essentially serves as a yield penalty compared to the other hybrids. It is recommended that plant development throughout the season and its effect on the cell wall content at the end of the growing season should be taken into consideration in future breeding efforts.

Biomass is evaluated from a quality perspective and therefore the cell wall composition is reported as the relative proportion of cellulose, hemicellulose, and lignin within the NDF fraction of the stems. Evaluation of the cell wall composition showed that generally the two types of seed-based hybrids ( $M. sin \times M. sin$  and  $M. sac \times M. sin$ ) remained distinguishable from each other and from the two clonally propagated genotypes (GRC 9 and GRC 15). The cell walls of the  $M. sin \times M. sin$  hybrids contained significantly less cellulose and more hemicellulose than those of  $M. sac \times M. sin$  origin. For  $M. sin \times M. sin$  hybrids, cellulose levels averaged 55.5% in 2021 and 55.6% in 2022, while  $M. sac \times M. sin$  hybrids and genotypes averaged 58.5% and 58.7% in 2021 and 2022, respectively. The differences within the group of  $M. sin \times M. sin$  hybrids were relatively small, the largest being 1.4% to 1.7% between GRC 1 and GRC 7. Within the group of  $M. sac \times M. sin$  hybrids, it stood out that  $M \times g$  had the highest amount of cellulose, although the difference appeared to be only significant in 2022 (Figure 2b). For  $M. sin \times M. sin$  hybrids, the average hemicellulose levels were 34.3% in 2021 and 34.7% in 2022. After the first growth year (2021) only a few significant differences

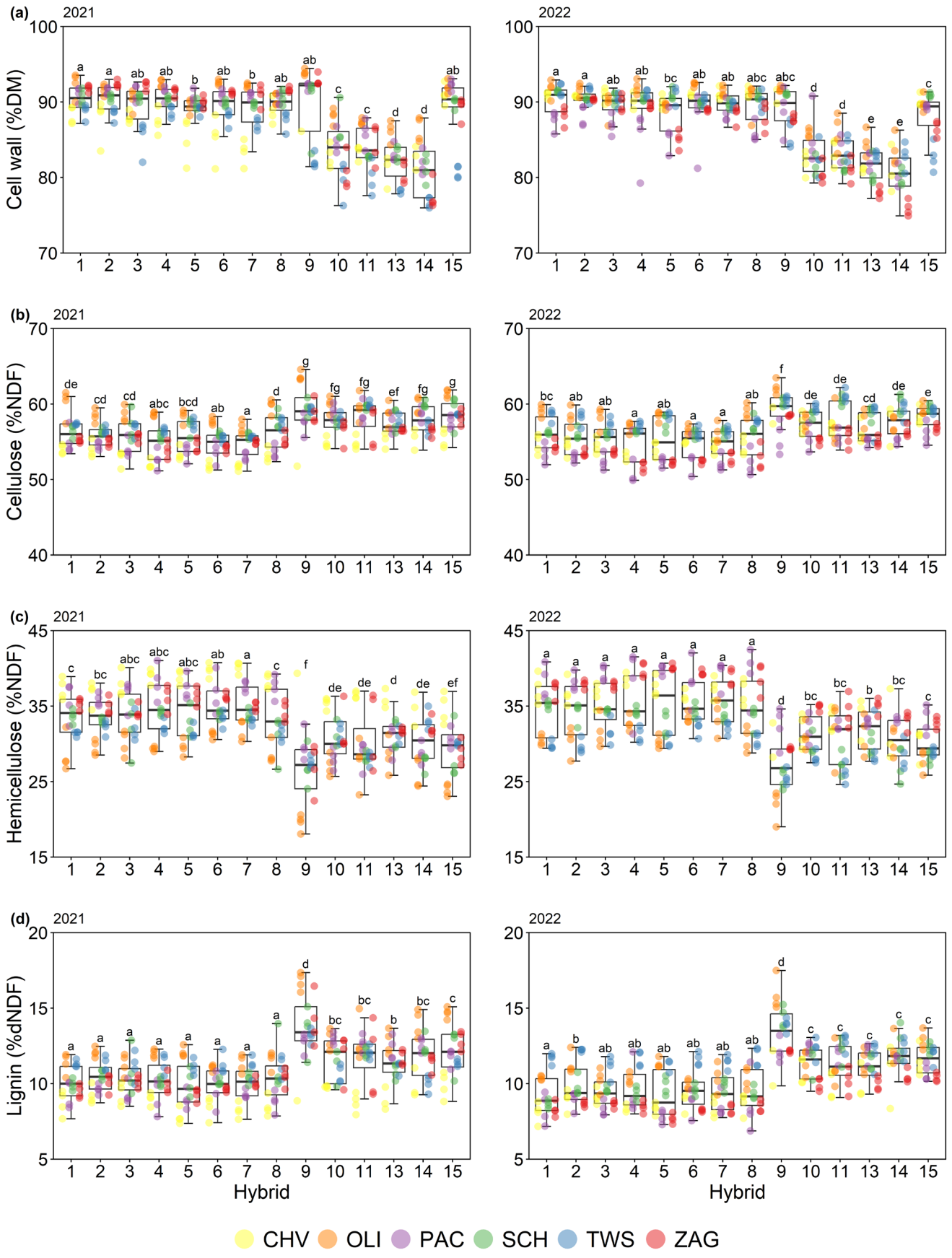


**FIGURE 2** | Cell wall content and composition of the seed-based *M. sin* × *M. sin* hybrids (GRC 1–8), *M* × *g* (GRC 9), seed-based *M. sac* × *M. sin* hybrids (GRC 10–11 and GRC 13–14) and the clonally propagated *M. sac* × *M. sin* hybrid (GRC 15) at the different trial locations, harvested in spring 2021 and spring 2022.

were found within this group of hybrids, while such differences were absent after the second growth season (Figure 2c). Hemicellulose levels of the seed-based *M. sac* × *M. sin* hybrids and GRC 15 ranged between 29.4% and 31.8% depending on the year. In here, only GRC 13 differed significantly from GRC 15 in both years. The differences in structural polysaccharides between *M. sin* × *M. sin* and *M. sac* × *M. sin* hybrids in this study might be originating from the individual breeding programs they have been selected from, as these traits are not necessarily distinct between species (Allison et al. 2011; Qin et al. 2012; Li, Pu, and Ragauskas 2016; Iacono et al. 2023). It stood out that *M* × *g* contained considerably less hemicellulose (26.7% in 2021 and 26.3% in 2022) compared to the seed-based hybrids in this study (Figure 2c). Higher cellulose levels and lower hemicellulose levels of *M* × *g*, relative to other *Miscanthus* species, have been reported previously (Hodgson et al. 2010; Allison et al. 2011; van der Weijde, Dolstra, et al. 2017).

Similar to the polysaccharides, the analysed hybrids displayed significant variation in lignin content, which was again mainly found between the *M. sin* × *M. sin* hybrids and the *M. sac* × *M. sin* hybrids. The *M. sin* × *M. sin* hybrids had an average lignin content of 10.2% in 2021 and 9.6% in 2022, which was significantly lower compared to 11.6% in 2021 and 11.3% in 2022 for seed-based *M. sac* × *M. sin* hybrids. However, in 2021, lignin content between these two groups was similar for samples from CHV, while lignin content was 0.3% lower in seed-based *M. sac* × *M. sin* hybrids compared to *M. sin* × *M. sin* hybrids from the trial at TWS (Figure 2d). The observation that seed-based *M. sac* × *M. sin* had the lowest lignin levels at TWS was unique. At the other four trial locations, the absolute lignin content of *M. sin* × *M. sin* hybrids was between 1.3% and 3.4% lower than that of the *M. sac* × *M. sin* hybrids in 2021. In contrast, in 2022, the *M. sin* × *M. sin* hybrids had a lower lignin content compared to that of the seed-based *M. sac* × *M. sin* hybrids at all trial locations. The lignin content of GRC15 was slightly higher (12.2% in 2021 and 11.7% in 2022) than that of the seed-based *M. sac* × *M. sin* hybrids. Multiple studies have reported lower lignin levels for *M. sinensis* compared to *M. sacchariflorus*, although a considerable range is present in both species (Allison et al. 2011; Qin et al. 2012; Li, Liao, et al. 2016). In both growth seasons, *M* × *g* contained the most lignin, averaging 13.9% in 2021 and 13.7% in 2022. The lignin content of *M* × *g* commonly exceeds that of other accessions and genotypes, and its high value can be considered a specific characteristic of this hybrid (Hodgson et al. 2010; Allison et al. 2011).

The observed similarities in cell wall composition within each group of inter- and intra-specific seed-based hybrids may be explained by the presence of genetic variation within these hybrids. Plants of the two clonally propagated hybrids (GRC 9 and GRC 15) were genetically uniform, while this was not the case for the seed-based hybrids. *Miscanthus* plants are self-incompatible, which prevents self-pollination and currently makes it impossible to create inbred lines that are required for genetically uniform F1 seed-hybrids (Sacks et al. 2013; Jiang et al. 2017). Instead, the creation of the seed-based hybrids relies on full-sib mating, and the resulting offspring will presumably show some degree of genetic variation (van der Crujisen et al. 2021), a source of variation absent in the two clonally propagated

genotypes. The impact of this additional source of variation was intended to be minimized by sampling five plants per plot. However, this number may have been too small to fully circumvent the plot-to-plot variation observed in the cell wall-related traits under study. Additionally, although the developed NIRS prediction models were highly accurate and comparable to those used in previous studies, there is still some degree of deviation between the predicted data from the model and the analyzed laboratory data (Hodgson et al. 2010; Huang et al. 2012; Payne and Wolfrum 2015; Jin et al. 2017; Kiesel et al. 2017; van der Weijde, Dolstra, et al. 2017). The external validations showed that predictions of ADL ( $R^2=0.76$ ) across multiple *Miscanthus* species were slightly more difficult compared to those of other components ( $R^2 \geq 0.90$ ), which has been reported before (Hodgson et al. 2010; Kiesel et al. 2017; van der Weijde, Dolstra, et al. 2017). Therefore, it is possible that some of the smaller differences became partly masked since ADL represents the lignin content and is also used in the calculation of cellulose. This lack of distinction between more subtle differences might explain the absence of variation within both groups of seed-based intra- and interspecific hybrids.

### 3.2 | Environmental Conditions Affect the Cell Wall Composition of Different Hybrids Similarly

The variation in cell wall content and its composition were not only determined by the genetic constitution of the hybrids, but also by the environmental conditions at each of the trial locations and growth years (Tables S2 and S3). For cell wall content, there was a much stronger interaction effect between location and year compared to the individual effects of these factors (Table S2). The cell wall content was the lowest at CHV and TWS in 2021 and PAC and ZAG in 2022, where it averaged between 84.3% and 86.3%. These values were significantly lower compared to those of the other growth year at these four locations (87.5%–89.1%), and also to the values that were observed for either year at OLI or SCH (Figure 3a). Similarly, the cell wall composition was considerably affected by the environmental conditions at the different trial locations and years. The average cellulose levels ranged between 57.4% and 59.4% at OLI, SCH, and TWS, which was significantly higher than the range from 53.6% to 55.8% at CHV, PAC, and ZAG (Figure 3b). The largest relative difference (10.8%) was observed between OLI (59.4%) and CHV (53.6%) in 2021. For hemicellulose, the opposite trend was observed, as it averaged between 33.3% and 37.4% at CHV, PAC, and ZAG, while its values ranged between 27.9% and 31.5% at OLI, SCH, and TWS (Figure 3c). The location effect applied to all hybrids, with the largest average difference in hemicellulose content being observed between CHV (37.4%) and OLI (27.9%) in 2021. In both growth seasons, lignin levels were relatively low at CHV (8.9% in 2021 and 9.4% in 2022). In contrast, plants at OLI in 2021 had on average a significantly higher lignin content (12.6%) than those at any of the other trial locations in that year. This was no longer true in 2022, as the average lignin content at OLI had decreased to 11.4%. The average lignin content also differed significantly between years at other trial locations, with relative differences of 7.8% at PAC, 6.5% at TWS, and 17.8% at ZAG. It was noteworthy that SCH was the only location where no significant differences in any of the cell wall components were observed between the two growth years. The ranges observed

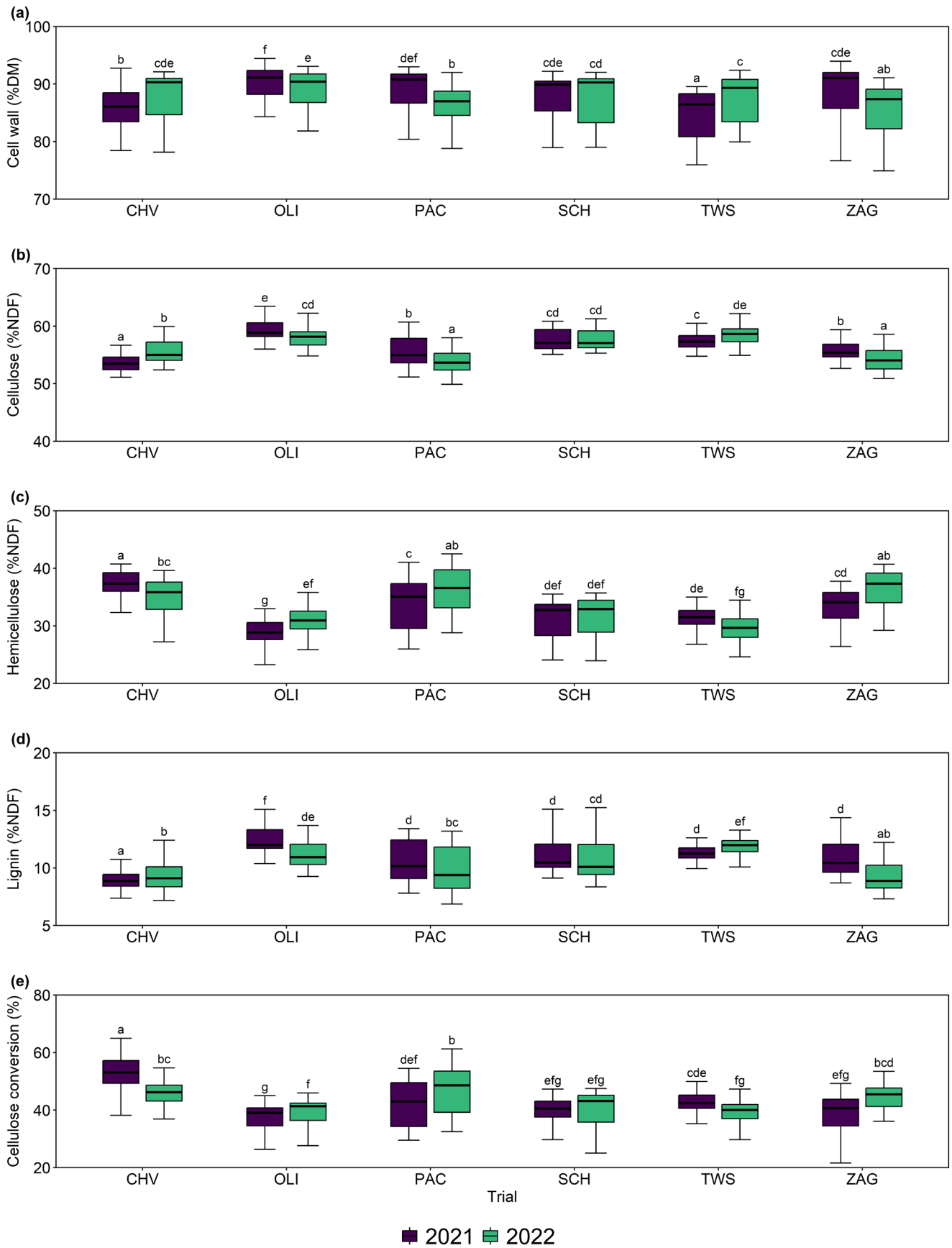


**FIGURE 3** | Cell wall content, composition, and cellulose conversion levels for the six trial locations in 2021 and 2022.

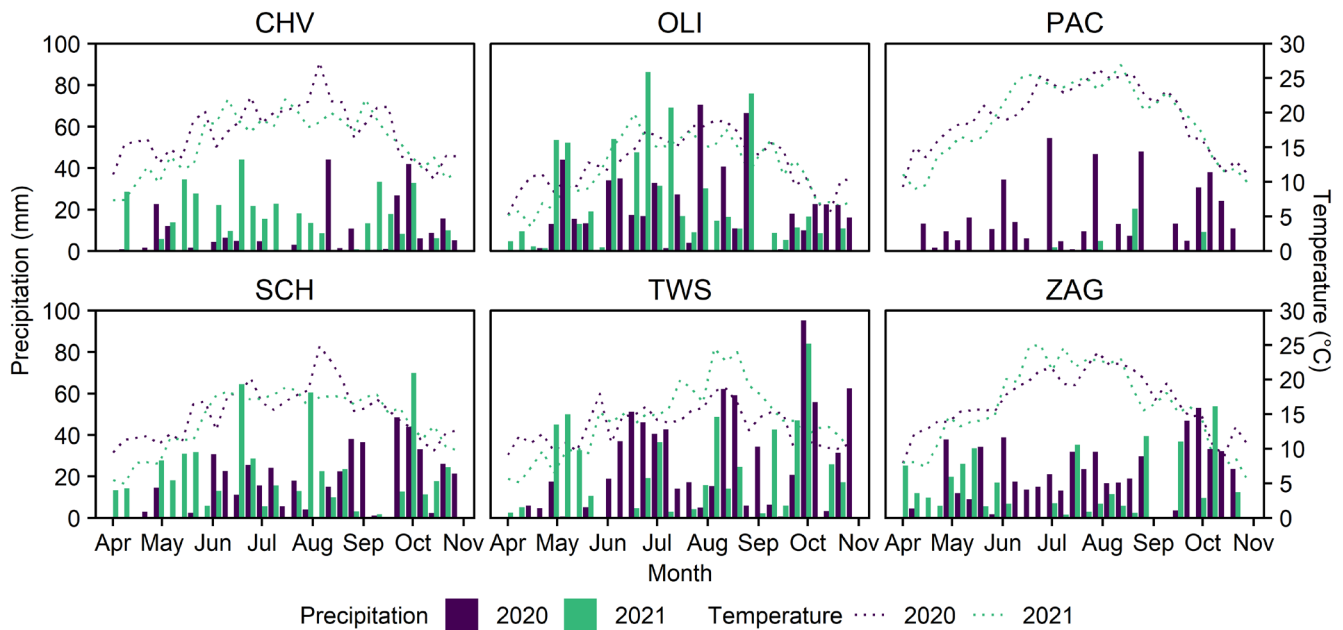


**FIGURE 4** | Precipitation and temperature per week during the growth season in 2020 and 2021 for the six trial locations.

for the different cell wall traits across locations were similar to those reported in previous multi-location trials across Europe (Hodgson et al. 2010; van der Weijde, Dolstra, et al. 2017).

Identifying factors determining variation between the cell walls of plants grown in different environments is often difficult, as under field conditions there are many complex interactions that together affect the cell wall composition. For instance, studies that have addressed the effect of a single abiotic stress showed that many external factors (e.g., temperature, wind, drought, heavy metal contamination, salinity) can modulate the cell wall composition (van der Weijde, Huxley, et al. 2017; Cheng et al. 2018; Gladala-Kostarz et al. 2020; de Freitas et al. 2022; van der Crujjsen et al. 2024). Each trial site in the current study had a unique environment that was largely defined by the combination of climatic conditions and important soil properties such as composition, water retention, and contamination (Awty-Carroll et al. 2022). For example, the soils at CHV and TWS were heavy metal contaminated to various degrees (Awty-Carroll et al. 2022) and exposure to heavy metals can affect virtually all the main cell wall components in plant stems (Cheng et al. 2018; Li et al. 2022; Yu et al. 2023). Nevertheless, it is difficult to disentangle the direct effect of these contaminants on the overall composition from the rest of the environment. Similarly, with the current data, it is unfeasible to dissect the variables that caused, for instance, the differences in cellulose content between locations or that would explain the high lignin content at OLI in 2021. However, for three locations, the strong location by year effects seem to be, at least partly, explained by drought occurring in one of the growth years.

Low amounts of precipitation combined with high temperatures led to drought at CHV in 2020, where from half of May until the end of July there was only 25.8 mm precipitation. The most extreme drought occurred at PAC in 2021, with only 3.4 mm precipitation between April until the end of July. In 2021 at ZAG, there was a 1.5-month period with little precipitation (21.4 mm)

between the start of June and the end of July (Figure 4). Although the drought spell at ZAG was relatively short compared to those of the other two locations, it still affected plant growth and significantly reduced their height compared to the previous year (Magenau et al. 2023). The years with severe drought spells had a significant reduction (2.8%–3.3%) in cell wall content. However, such reductions were not observed for the seed-based *M. sac* × *M. sin* hybrids in the dry year at the CHV trial. Although cellulose levels were already lower at CHV, PAC, and ZAG compared to the three other trial locations, they declined further (2.8%–3.6%) in the years when drought occurred, likely explaining to some extent the significant interaction between location and year (Table S3). In contrast, hemicellulose increased significantly (6.8%–9.6%) at all three trials that experienced drought compared to the non-drought year. Lignin was also affected by the lack of precipitation, as drought significantly reduced its content by 5.3% at CHV, 7.8% at PAC, and 17.8% at ZAG compared to the non-drought year.

Although there was some variation in the extent to which the cell wall components of specific hybrids were affected within a single location, this variation was not consistently observed across the drought-affected locations. Thus, we can conclude that although a generally similar response was observed for all hybrids, exceptions may occur under specific conditions. Reductions in cell wall content, cellulose, and lignin, which coincided with increased hemicellulose levels, have all been reported as consequences of exposure to drought in miscanthus (van der Weijde, Huxley, et al. 2017; Hoover et al. 2018). Therefore, it is likely that these changes can indeed be assigned to drought since the same pattern was also consistently observed in multiple locations that experienced drought. In the current study, three out of 12 trial environments were affected by drought due to a combination of lack of precipitation and high temperatures. It is anticipated that droughts of this nature will occur with increasing frequency in Europe in the near future (Yuan et al. 2023; Zeng et al. 2023). Miscanthus cultivation is likely to be affected by such droughts

as for economic reasons it is rain-fed rather than irrigated and is unlikely to be prioritized over food crops when the availability of water is low (Clifton-Brown and Lewandowski 2000; Xie et al. 2019). It is important to realize that whether the compositional changes induced by drought would be favorable or detrimental properties depends entirely on the intended end use of the biomass. Therefore, the development of miscanthus varieties that are resilient towards drought and maintain a stable cell wall composition is desirable.

### 3.3 | Novel Hybrids Outperformed $M \times g$ in Terms of Cellulose Conversion and Potential Ethanol Yields

Cellulose conversion is defined as the percentage of cellulose that was hydrolyzed into glucose monomers during the enzymatic saccharification process. The cellulose conversion levels were the highest for GRC 1–8, averaging 45.2% in both growth years. Conversion levels for seed-based  $M. sac \times M. sin$  were significantly lower, averaging 39.2% in 2021 and 39.1% in 2022. GRC 15 had slightly lower conversion levels (36.6% in 2021 and 37.5% in 2022) than those of seed-based  $M. sac \times M. sin$ , although these differences were mostly not significant. In contrast, the cellulose conversion levels of  $M \times g$  were significantly lower compared to any of the other hybrids, averaging 32.0% in 2021 and 31.7% in 2022 (Figure 5a). Although the average cellulose conversion levels across all locations appeared to be rather similar between both growth years, this was not the case for individual environments. First, the general observation that  $M. sin \times M. sin$  hybrids achieved the highest cellulose conversion rates was true in all environments with the exception of TWS in 2021. In

this location, the seed-based  $M. sac \times M. sin$  hybrids (GRC 10–11, GRC 13–14) outperformed the  $M. sin \times M. sin$  (GRC 1–8) hybrids by 4.3% on average. Furthermore, the average cellulose conversion levels differed significantly between growth years at every location with the exception of SCH. During the drought years at CHV, PAC, and ZAG, cellulose conversion increased by 10.5%–16.4% relative to the non-drought year. This agrees with the findings of Hoover et al. (2018) that drought-induced cell wall modulation in  $M \times g$  made its biomass less recalcitrant to degradation. In comparison, the relative differences in cellulose conversion between both years at OLI (5.5%), SCH (2.5%) and TWS (7.7%) were smaller.

The location-to-location and year-to-year differences were indicated by the statistical analysis (Table S2), but also expected given that achievable cellulose conversion levels largely depend on the cell wall composition. Cellulose conversion was negatively correlated to lignin ( $r = -0.91$ ) and cellulose ( $r = -0.81$ ), while it correlated positively to hemicellulose ( $r = 0.88$ ). These correlations were in line with values previously reported (Belmokhtar et al. 2017; van der Weijde, Kiesel, et al. 2017) and can be explained by the unique structural properties of each component. High lignin levels constitute the main barrier for efficient cellulose conversion, as they protect cellulose fibrils and prevent the enzymes from hydrolyzing them (Li, Liao, et al. 2016). In addition, previous studies have reported that miscanthus plants with higher cellulose levels often have a higher level of crystallinity, while the presence of hemicellulose tends to decrease cellulose crystallinity (Xu et al. 2012; Li et al. 2013). The organized structure of crystalline cellulose limits enzymatic accessibility and thereby has a negative effect on saccharification efficiency

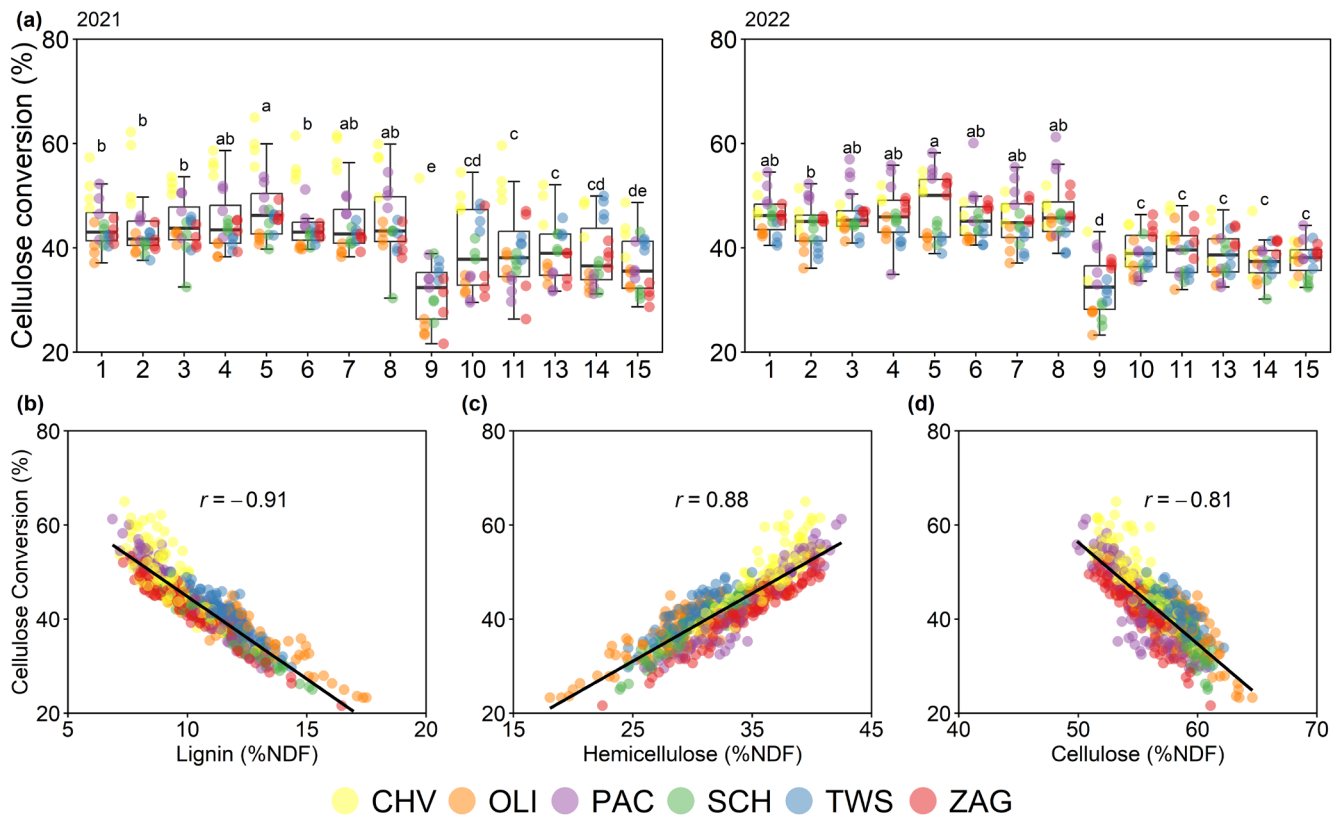


**FIGURE 5** | Cellulose conversion for the miscanthus hybrids at the six trial locations in 2021 and 2022 (a). Correlations between cellulose conversion and cell wall components (b).

(Yoshida et al. 2008; Zhang et al. 2013). Another consideration from our results is that plants with lower lignin levels, resulting from either genetic factors or environmental conditions, always had reduced cellulose levels and increased hemicellulose levels, and vice versa. These observations explain both the high correlations existing between each of the cell wall components (Figure S1) and the high correlations of each component with cellulose conversion (Figure 5b).

The potential ethanol yields of each hybrid depend on the cellulose content within the cell walls, the enzymatic conversion efficiency of cellulose to glucose, and the overall stem yield. Stem yields at the six trial locations were determined after the third growing season, indicating they should generally be representative for those in mature stands (Arnoult et al. 2015; Kalinina et al. 2017). The average stem yield of  $M \times g$  varied between  $588 \text{ g m}^{-2}$  and  $1532 \text{ g m}^{-2}$  at TWS, PAC, ZAG, and OLI. For indicative purposes,  $M \times g$  plants from the adjacent trial at SCH yielded on average  $1950 \text{ g m}^{-2}$  (Figure S2). These averages show that, although with considerable variation between plots, only at OLI (and likely at SCH)  $M \times g$  achieved the high yields that have been regularly reported in the literature (Clifton-Brown et al. 2001; Zub et al. 2011; Gauder et al. 2012). Yields at the lower end of the spectrum might be explained by the harsh growing conditions on marginal lands, such as less favorable soil conditions and structure (Magenau et al. 2022). However, large variations in yield between locations are also not unique for  $M \times g$ , and the current results fall well within the broader ranges reported elsewhere (Lesur-Dumoulin et al. 2016; Shepherd et al. 2020).

Yields of the other experimental hybrids also varied considerably between trials, and there was no single hybrid that outperformed all the others in terms of yield at every location (Figure S2). It stood out that the highest average yields at each location, except for CHV, were all achieved by  $M. sac \times M. sin$  hybrids, which ranged from  $1224 \text{ g m}^{-2}$  (GRC 15, ZAG) to  $1848 \text{ g m}^{-2}$  (GRC 15, SCH). In comparison, the best performing  $M. sin \times M. sin$  hybrid at each location yielded between  $962 \text{ g m}^{-2}$  (GRC 7, ZAG) and  $1246 \text{ g m}^{-2}$  (GRC 8, SCH). The doubled planting density for  $M. sin \times M. sin$  hybrids was intended to compensate for their smaller stature, although a recent study provided no evidence that doubling the planting density would indeed lead to increased yields in  $M. sinensis$  (Ouattara et al. 2020). For all hybrids, stem weights varied considerably between the individual plants within each plot, which also led to a large within-group variance in estimated means per plot. Consequently, although there appeared to be considerable variation between the average yields of hybrids within each location, these differences were rarely found to be significant (Figure S2). Yield measurements were averaged over five plants per plot, which might still be too small in surface area and plant number to sufficiently reduce between-plot variance for reliable yield assessments in miscanthus (Knörzer et al. 2013). Nevertheless, even over a larger surface area, it remained difficult to significantly distinguish these hybrids based on their third year yields (Awty-Carroll et al. 2022). The lack of significant differences indicates that in most of these trials, seed-based hybrids achieved comparable yields to those of  $M \times g$ .

Since yield differences were generally not significant, it means that performance in terms of theoretical ethanol yields would

largely depend on the availability of cellulose and the achievable cellulose conversion rates. Considering the amount of cellulose, it stood out that seed-based  $M. sac \times M. sin$  hybrids contained on average 7.7%–10.0% less cell walls compared to the other hybrids. Consequently, although these hybrids exhibit a high cellulose content within the NDF fraction, their cellulose content per gram of dry matter is lower compared to most other hybrids evaluated in this study (Figure S3). On average, the highest availability of cellulose was achieved by  $M \times g$  and GRC 15, as they combined high cell wall content with high cellulose levels. In contrast, the highest cellulose conversion levels were achieved by the  $M. sin \times M. sin$  hybrids. If stem yields are considered equal and cellulose levels and conversion are taken into account, the theoretical ethanol yields of  $M. sin \times M. sin$  hybrids would be 32.9% higher compared to  $M \times g$ . The seed-based  $M. sac \times M. sin$  and GRC15 would yield 9.8% and 13.1% more ethanol compared to  $M \times g$  under the same assumptions (Figure 6). Thus,  $M \times g$  needs to achieve considerably higher biomass yields compared to the other hybrids to match their theoretical ethanol output.

Since  $M \times g$  did not achieve significantly higher stem yields at any of the trial locations, these findings suggest that under all conditions, other hybrids performed better in terms of theoretical ethanol yields. However, it is important to consider that when focusing solely on averages, the yields of  $M \times g$  at OLI and SCH surpassed those of the most productive seed-based  $M. sin \times M. sin$  hybrids by 36.4% and 56.5%, respectively. Furthermore, when compared to the highest yielding seed-based  $M. sac \times M. sin$  hybrids, the yield of  $M \times g$  was 25.1% higher at OLI and 42.1% higher at SCH. Thus, although the observed differences were not significant, it does appear that  $M \times g$  had a yield advantage in these two locations. However, in both locations, the yields of  $M \times g$  were roughly equal to those of GRC 15, indicating that the latter would be the best prospect for ethanol yields. Also, the reported cellulose

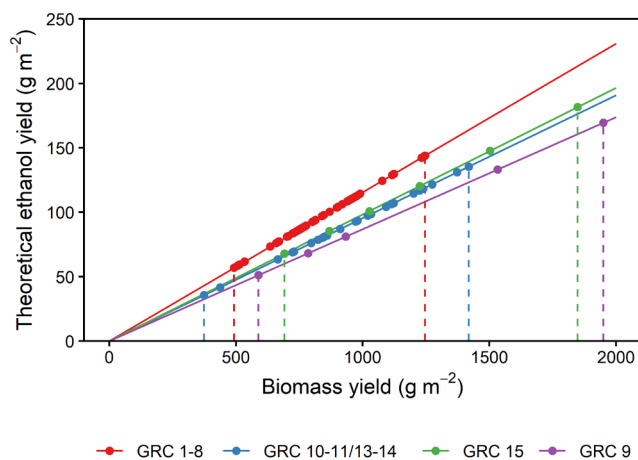


**FIGURE 6** | Theoretical ethanol yield based on the average biomass yield in the third growing season (harvested spring 2021) from each hybrid per trial location. GRC 1–8: Seed-based  $M. sin \times M. sin$  hybrids, GRC 9:  $M \times g$ , GRC 10–11/13–14: Seed-based  $M. sac \times M. sin$  hybrids, GRC 15: Clonally propagated  $M. sac \times M. sin$ . Calculations of ethanol yield were based on the averaged cellulose content and cellulose conversion rates across trials and years for each of the specified GRC-hybrid subsets. Vertically dashed lines indicate the observed ranges per subset.

conversion levels are only valid for the experimental conditions used in this study, where pretreatment intensity was moderate, as it allows discrimination between hybrids (van der Weijde, Kiesel, et al. 2017). Nevertheless, several studies have illustrated that a more amenable cell wall composition also increased saccharification efficiency and ethanol production in larger scale testing facilities that more closely resemble full-scale production plants (Belmokhtar et al. 2017; Cerazy-Waliszewska et al. 2019; Bhatia et al. 2020). For instance, Cerazy-Waliszewska et al. (2019) also reported higher polysaccharide conversion rates for *M. sin* (83% and 86%) compared to *M×g* (62% and 76%). However, in their study, the yields of *M×g* (21.5 t ha<sup>-1</sup>) were significantly higher than those of *M. sin* (17.0 t ha<sup>-1</sup>), leading to slight differences in estimated ethanol levels. Regarding yield, it was clear that *M×g* struggled to reach its potential yields at most of the trial locations. A previous study on mostly arable lands revealed that although *M×g* performed relatively well in terms of yield, it was still often matched or even surpassed by other accessions and genotypes (Kalinina et al. 2017). Additionally, these other accessions and genotypes also had higher theoretical ethanol yields (van der Weijde, Dolstra, et al. 2017). Higher yields positively impact the production of ethanol and methane from a sustainability point of view and are also critical for economic viability (Lask et al. 2019; Wagner et al. 2019; Adler 2023). Both current and past findings highlight that certain miscanthus hybrids have the potential to outperform *M×g* in terms of projected ethanol yields, especially when cultivated on marginal lands. Therefore, depending on the specific environment and potential end-uses of the biomass, it would be beneficial to carefully consider these alternative miscanthus hybrids instead of *M×g* when establishing new cultivation areas.

## 4 | Conclusion

The purpose of this study was to evaluate how recently developed miscanthus hybrids would compare to *M×g* when cultivated on marginal lands in terms of yield, cell wall composition, and suitability for bioconversion into ethanol. The results showed that in most environments, *M×g* struggled to obtain significantly higher yields under sub-optimal environmental conditions compared to the novel hybrids. The seed-based *M. sac* × *M. sin* hybrids accumulated less cell wall compared to the other hybrids. This was likely due to their late maturation, which had a negative impact as it lowered the absolute amount of cell wall components per gram of dry matter. The cell wall composition of the seed-based hybrids differed significantly from that of *M×g*, resulting in higher cellulose conversion levels for the seed-based hybrids. In particular, the cell wall composition of the *M. sin* × *M. sin* hybrids was beneficial for conversion, which under certain conditions could largely compensate for their lower biomass yield potential. Considering all aspects of performance, either the seed-based hybrids or GRC 15 would have achieved higher theoretical ethanol yields compared to *M×g* in each of the evaluated environments. Although *M×g* remains the most widely cultivated miscanthus genotype, replacing it with improved varieties would be more beneficial for bioethanol production on marginal lands. Further breeding efforts would likely lead to new varieties better adapted to challenging conditions and suitable for other dedicated end-uses.

## Author Contributions

**Kasper van der Crujzen:** conceptualization, data curation, investigation, validation, visualization, writing – original draft. **Mohamad Al Hassan:** conceptualization, data curation, investigation, writing – original draft. **Oene Dolstra:** conceptualization, formal analysis, investigation, resources, writing – original draft. **Elena Magenau:** investigation, resources. **Mislav Kontek:** investigation, resources. **Chris Ashman:** investigation, resources. **Danny Awty-Carroll:** investigation, resources. **Andrea Ferrarini:** investigation, resources. **Enrico Martani:** resources. **Phillip van der Pluijm:** resources. **Gert-Jan Petri:** resources. **Emmanuel de Maupeou:** resources. **Maria-João Paulo:** formal analysis. **Jason Kam:** resources. **Bert-Jan van Dinter:** resources. **Lars Kraak:** resources. **Annemarie Dechesne:** investigation, methodology. **Vanja Jurišić:** resources. **Iris Lewandowski:** funding acquisition, resources, writing – review and editing. **Stefano Amaducci:** writing – review and editing. **John Clifton-Brown:** resources, writing – review and editing. **Andreas Kiesel:** project administration, writing – review and editing. **Luisa M. Trindade:** conceptualization, funding acquisition, project administration, resources, supervision, writing – original draft.

## Acknowledgments

We would like to thank all staff that were involved with planting, maintenance, and harvesting of the trials, and Gerrit Huisman, Wim van der Slikke, and Dafydd Timmerman for their assistance with processing the harvested biomass.

## Conflicts of Interest

The authors declare no conflicts of interest.

## Data Availability Statement

The data that support the findings of this study are openly available in figshare at <https://doi.org/10.6084/m9.figshare.29361626>.

## References

- Adler, P. R. 2023. "Life Cycle Inventory of Miscanthus Production on a Commercial Farm in the US." *Frontiers in Plant Science* 14: 1029141. <https://doi.org/10.3389/fpls.2023.1029141>.
- Allison, G. G., C. Morris, J. Clifton-Brown, S. J. Lister, and I. S. Donnison. 2011. "Genotypic Variation in Cell Wall Composition in a Diverse Set of 244 Accessions of Miscanthus." *Biomass and Bioenergy* 35: 4740–4747. <https://doi.org/10.1016/j.biombioe.2011.10.008>.
- Amaducci, S., G. Facciotto, S. Bergante, et al. 2017. "Biomass Production and Energy Balance of Herbaceous and Woody Crops on Marginal Soils in the Po Valley." *GCB Bioenergy* 9: 31–45. <https://doi.org/10.1111/gcbb.12341>.
- Arnoult, S., M. C. Mansard, and M. Brancourt-Hulmel. 2015. "Early Prediction of Miscanthus Biomass Production and Composition Based on the First Six Years of Cultivation." *Crop Science* 55: 1104–1116. <https://doi.org/10.2135/cropsci2014.07.0493>.
- Awty-Carroll, D., E. Magenau, M. Al Hassan, et al. 2022. "Yield Performance of Fourteen Novel Inter- and Intra-Species Miscanthus Hybrids Across Europe." 15: 399–423. <https://doi.org/10.1111/gcbb.13026>.
- Bates, D., M. Mächler, B. Bolker, and S. Walker. 2015. "Fitting Linear Mixed-Effects Models Using lme4." *Journal of Statistical Software* 67: 1–48. <https://doi.org/10.18637/jss.v067.i01>.
- Belmokhtar, N., S. Arnoult, B. Chabbert, J. P. Charpentier, and M. Brancourt-Hulmel. 2017. "Saccharification Performances of Miscanthus at the Pilot and Miniaturized Assay Scales: Genotype and

- Year Variabilities According to the Biomass Composition." *Frontiers in Plant Science* 8: 1–13. <https://doi.org/10.3389/fpls.2017.00740>.
- Bhatia, R., A. Winters, D. N. Bryant, et al. 2020. "Pilot-Scale Production of Xylo-Oligosaccharides and Fermentable Sugars From *Miscanthus* Using Steam Explosion Pretreatment." *Bioresource Technology* 296: 122285. <https://doi.org/10.1016/j.biortech.2019.122285>.
- Boakye-Boaten, N. A., L. Kurkalova, S. Xiu, and A. Shahbazi. 2017. "Techno-Economic Analysis for the Biochemical Conversion of *Miscanthus x Giganteus* Into Bioethanol." *Biomass and Bioenergy* 98: 85–94. <https://doi.org/10.1016/j.biombioe.2017.01.017>.
- Cerazy-Waliszewska, J., S. Jeżowski, P. Łysakowski, et al. 2019. "Potential of Bioethanol Production From Biomass of Various *Miscanthus* Genotypes Cultivated in Three-Year Plantations in West-Central Poland." *Industrial Crops and Products* 141: 111790.
- Cheng, S., H. Yu, M. Hu, et al. 2018. "Miscanthus Accessions Distinctively Accumulate Cadmium for Largely Enhanced Biomass Enzymatic Saccharification by Increasing Hemicellulose and Pectin and Reducing Cellulose CrI and DP." *Bioresource Technology* 263: 67–74. <https://doi.org/10.1016/j.biortech.2018.04.031>.
- Clark, L. v., M. S. Dwiyantri, K. G. Anzoua, et al. 2019. "Biomass Yield in a Genetically Diverse *Miscanthus sinensis* Germplasm Panel Evaluated at Five Locations Revealed Individuals With Exceptional Potential." *GCB Bioenergy* 11: 1125–1145. <https://doi.org/10.1111/gcbb.12606>.
- Clifton-Brown, J., A. Hastings, M. Mos, et al. 2017. "Progress in Upscaling *Miscanthus* Biomass Production for the European Bio-Economy With Seed-Based Hybrids." *GCB Bioenergy* 9: 6–17. <https://doi.org/10.1111/gcbb.12357>.
- Clifton-Brown, J. C., and I. Lewandowski. 2000. "Water Use Efficiency and Biomass Partitioning of Three Different *Miscanthus* Genotypes With Limited and Unlimited Water Supply." *Annals of Botany* 86: 191–200. <https://doi.org/10.1006/anbo.2000.1183>.
- Clifton-Brown, J. C., I. Lewandowski, B. Andersson, et al. 2001. "Performance of 15 *Miscanthus* Genotypes at Five Sites in Europe." *Agronomy Journal* 93: 1013–1019. <https://doi.org/10.2134/agronj2001.9351013x>.
- Cunha, J. T., A. Romani, C. E. Costa, I. Sá-Correia, and L. Domingues. 2019. "Molecular and Physiological Basis of *Saccharomyces cerevisiae* Tolerance to Adverse Lignocellulose-Based Process Conditions." *Applied Microbiology and Biotechnology* 103: 159–175. <https://doi.org/10.1007/s00253-018-9478-3>.
- da Costa, R. M. F., R. Simister, L. A. Roberts, et al. 2018. "Nutrient and Drought Stress: Implications for Phenology and Biomass Quality in *Miscanthus*." *Annals of Botany* 124, no. 4: 1–566. <https://doi.org/10.1093/aob/mcy155>.
- de Freitas, E. N., V. Khatri, D. R. Contin, et al. 2022. "Climate Change Affects Cell-Wall Structure and Hydrolytic Performance of a Perennial Grass as an Energy Crop." *Biofuels, Bioproducts and Biorefining* 16: 471–487. <https://doi.org/10.1002/bbb.2312>.
- Gauder, M., S. Graeff-Hönninger, I. Lewandowski, and W. Claupein. 2012. "Long-Term Yield and Performance of 15 Different *Miscanthus* Genotypes in Southwest Germany." *Annals of Applied Biology* 160: 126–136. <https://doi.org/10.1111/j.1744-7348.2011.00526.x>.
- Gladala-Kostarz, A., J. H. Doonan, and M. Bosch. 2020. "Mechanical Stimulation in *Brachypodium distachyon*: Implications for Fitness, Productivity, and Cell Wall Properties." *Plant, Cell & Environment* 43: 1314–1330. <https://doi.org/10.1111/pce.13724>.
- Głowacka, K., L. V. Clark, S. Adhikari, et al. 2015. "Genetic Variation in *Miscanthus x Giganteus* and the Importance of Estimating Genetic Distance Thresholds for Differentiating Clones." *GCB Bioenergy* 7: 386–404. <https://doi.org/10.1111/gcbb.12166>.
- Godin, B., S. Lamaudière, R. Agneessens, et al. 2013. "Chemical Characteristics and Biofuels Potentials of Various Plant Biomasses: Influence of the Harvesting Date." *Journal of the Science of Food and Agriculture* 93: 3216–3224. <https://doi.org/10.1002/jsfa.6159>.
- He, L., C. Wang, H. Shi, W. Zhou, Q. Zhang, and X. Chen. 2019. "Combination of Steam Explosion Pretreatment and Anaerobic Alkalization Treatment to Improve Enzymatic Hydrolysis of *Hippophae rhamnoides*." *Bioresource Technology* 289: 121693. <https://doi.org/10.1016/j.biortech.2019.121693>.
- Hodgson, E. M., S. J. Lister, A. V. Bridgwater, J. Clifton-Brown, and I. S. Donnison. 2010. "Genotypic and Environmentally Derived Variation in the Cell Wall Composition of *Miscanthus* in Relation to Its Use as a Biomass Feedstock." *Biomass and Bioenergy* 34: 652–660. <https://doi.org/10.1016/j.biombioe.2010.01.008>.
- Hoover, A., R. Emerson, A. Ray, et al. 2018. "Impact of Drought on Chemical Composition and Sugar Yields From Dilute-Acid Pretreatment and Enzymatic Hydrolysis of *Miscanthus*, a Tall Fescue Mixture, and Switchgrass." *Frontiers in Energy Research* 6: 1–15. <https://doi.org/10.3389/fenrg.2018.00054>.
- Hu, R., Y. Xu, C. Yu, et al. 2017. "Transcriptome Analysis of Genes Involved in Secondary Cell Wall Biosynthesis in Developing Internodes of *Miscanthus lutarioriparius*." *Scientific Reports* 7: 9034. <https://doi.org/10.1038/s41598-017-08690-8>.
- Huang, J., T. Xia, A. Li, et al. 2012. "A Rapid and Consistent Near Infrared Spectroscopic Assay for Biomass Enzymatic Digestibility Upon Various Physical and Chemical Pretreatments in *Miscanthus*." *Bioresource Technology* 121: 274–281. <https://doi.org/10.1016/j.biortech.2012.06.015>.
- Iacono, R., G. T. Slavov, C. L. Davey, J. Clifton-Brown, G. Allison, and M. Bosch. 2023. "Variability of Cell Wall Recalcitrance and Composition in Genotypes of *Miscanthus* From Different Genetic Groups and Geographical Origin." *Frontiers in Plant Science* 14: 1155188. <https://doi.org/10.3389/fpls.2023.1155188>.
- Jensen, E., P. Robson, K. Farrar, et al. 2017. "Towards *Miscanthus* Combustion Quality Improvement: The Role of Flowering and Senescence." *GCB Bioenergy* 9: 891–908. <https://doi.org/10.1111/gcbb.12391>.
- Jeżowski, S., M. Mos, S. Buckby, et al. 2017. "Establishment, Growth, and Yield Potential of the Perennial Grass *Miscanthus x Giganteus* on Degraded Coal Mine Soils." *Frontiers in Plant Science* 8: 1–8. <https://doi.org/10.3389/fpls.2017.00726>.
- Jiang, J., Y. Guan, S. McCormick, J. Juvik, T. Lubberstedt, and S. Z. Fei. 2017. "Gametophytic Self-Incompatibility Is Operative in *Miscanthus sinensis* (Poaceae) and Is Affected by Pistil Age." *Crop Science* 57: 1948–1956. <https://doi.org/10.2135/cropsci2016.11.0932>.
- Jin, X., X. Chen, C. Shi, et al. 2017. "Determination of Hemicellulose, Cellulose and Lignin Content Using Visible and Near Infrared Spectroscopy in *Miscanthus sinensis*." *Bioresource Technology* 241: 603–609. <https://doi.org/10.1016/j.biortech.2017.05.047>.
- Jung, H. G., and M. D. Casler. 2006. "Maize Stem Tissues: Cell Wall Concentration and Composition During Development." *Crop Science* 46: 1793–1800. <https://doi.org/10.2135/cropsci2005.02-0085>.
- Kalinina, O., C. Nunn, R. Sanderson, et al. 2017. "Extending *Miscanthus* Cultivation With Novel Germplasm at Six Contrasting Sites." *Frontiers in Plant Science* 8: 1–15. <https://doi.org/10.3389/fpls.2017.00563>.
- Kiesel, A., C. Nunn, Y. Iqbal, et al. 2017. "Site-Specific Management of *Miscanthus* Genotypes for Combustion and Anaerobic Digestion: A Comparison of Energy Yields." *Frontiers in Plant Science* 8: 1–15. <https://doi.org/10.3389/fpls.2017.00347>.
- Knörzer, H., K. Hartung, H. P. Piepho, and I. Lewandowski. 2013. "Assessment of Variability in Biomass Yield and Quality: What Is an Adequate Size of Sampling Area for *Miscanthus*?" *GCB Bioenergy* 5: 572–579. <https://doi.org/10.1111/gcbb.12027>.

- Kuznetsova, A., P. B. Brockhoff, and R. H. B. Christensen. 2017. "lmerTest Package: Tests in Linear Mixed Effects Models." *Journal of Statistical Software* 82, no. 13: 1–26. <https://doi.org/10.18637/JSS.V082.I13>.
- Lask, J., M. Wagner, L. M. Trindade, and I. Lewandowski. 2019. "Life Cycle Assessment of Ethanol Production From Miscanthus: A Comparison of Production Pathways at Two European Sites." *GCB Bioenergy* 11: 269–288. <https://doi.org/10.1111/gcbb.12551>.
- Lenth, R. 2025. "emmeans: Estimated Marginal Means, aka Least-Squares Means." R Package Version 1.11.1-00001. <https://rvlenth.github.io/emmeans/>.
- Lesur-Dumoulin, C., M. Lorin, M. Bazot, M. H. Jeuffroy, and C. Loyce. 2016. "Analysis of Young Miscanthus × Giganteus Yield Variability: A Survey of Farmers' Fields in East Central France." *GCB Bioenergy* 8: 122–135. <https://doi.org/10.1111/gcbb.12247>.
- Li, F., S. Ren, W. Zhang, et al. 2013. "Arabinose Substitution Degree in Xylan Positively Affects Lignocellulose Enzymatic Digestibility After Various NaOH/H<sub>2</sub>SO<sub>4</sub> Pretreatments in Miscanthus." *Bioresource Technology* 130: 629–637. <https://doi.org/10.1016/j.biortech.2012.12.107>.
- Li, M., Y. Pu, and A. J. Ragauskas. 2016. "Current Understanding of the Correlation of Lignin Structure With Biomass Recalcitrance." *Frontiers in Chemistry* 4: 1–8. <https://doi.org/10.3389/fchem.2016.00045>.
- Li, R., Y. Zhao, Z. Sun, et al. 2022. "Genome-Wide Identification of Switchgrass Laccases Involved in Lignin Biosynthesis and Heavy-Metal Responses." *International Journal of Molecular Sciences* 23: 6530.
- Li, X., H. Liao, C. Fan, et al. 2016. "Distinct Geographical Distribution of the Miscanthus Accessions With Varied Biomass Enzymatic Saccharification." *PLoS One* 11: 1–15. <https://doi.org/10.1371/journal.pone.0160026>.
- Limayem, A., and S. C. Ricke. 2012. "Lignocellulosic Biomass for Bioethanol Production: Current Perspectives, Potential Issues and Future Prospects." *Progress in Energy and Combustion Science* 38: 449–467. <https://doi.org/10.1016/j.pecc.2012.03.002>.
- Magenau, E., J. Clifton-Brown, D. Awty-Carroll, et al. 2022. "Site Impacts Nutrient Translocation Efficiency in Intraspecies and Interspecies Miscanthus Hybrids on Marginal Lands." *GCB Bioenergy* 14: 1035–1054. <https://doi.org/10.1111/gcbb.12985>.
- Magenau, E., J. Clifton-Brown, C. Parry, et al. 2023. "Spring Emergence and Canopy Development Strategies in Miscanthus Hybrids in Mediterranean, Continental and Maritime European Climates." 15: 559–574. <https://doi.org/10.1111/gcbb.13035>.
- Matos, D. A., I. P. Whitney, M. J. Harrington, and S. P. Hazen. 2013. "Cell Walls and the Developmental Anatomy of the *Brachypodium distachyon* Stem Internode." *PLoS One* 8: e80640. <https://doi.org/10.1371/journal.pone.0080640>.
- Quattara, M. S., A. Laurent, C. Barbu, et al. 2020. "Effects of Several Establishment Modes of Miscanthus × Giganteus and *Miscanthus sinensis* on Yields and Yield Trends." *GCB Bioenergy* 12: 524–538. <https://doi.org/10.1111/gcbb.12692>.
- Payne, C. E., and E. J. Wolfrum. 2015. "Rapid Analysis of Composition and Reactivity in Cellulosic Biomass Feedstocks With Near-Infrared Spectroscopy." *Biotechnology for Biofuels* 8: 43. <https://doi.org/10.1186/s13068-015-0222-2>.
- Qin, J., Y. Yang, J. Jiang, et al. 2012. "Comparison of Lignocellulose Composition in Four Major Species of Miscanthus." *African Journal of Biotechnology* 11: 12529–12537. <https://doi.org/10.5897/ajb11.3248>.
- Quinn, L. D., K. C. Straker, J. Guo, et al. 2015. "Stress-Tolerant Feedstocks for Sustainable Bioenergy Production on Marginal Land." *Bioenergy Research* 8: 1081–1100. <https://doi.org/10.1007/s12155-014-9557-y>.
- Rancour, D. M., J. M. Marita, and R. D. Hatfield. 2012. "Cell Wall Composition Throughout Development for the Model Grass *Brachypodium distachyon*." *Frontiers in Plant Science* 3: 1–14. <https://doi.org/10.3389/fpls.2012.00266>.
- Sacks, E. J., J. A. Juvik, Q. Lin, J. R. Stewart, and T. Yamada. 2013. "The Gene Pool of Miscanthus Species and Its Improvement." In *Genomics of the Saccharinae*, edited by A. H. Paterson, 73–101. Springer New York. [https://doi.org/10.1007/978-1-4419-5947-8\\_4](https://doi.org/10.1007/978-1-4419-5947-8_4).
- Sarath, G., L. M. Baird, K. P. Vogel, and R. B. Mitchell. 2007. "Internode Structure and Cell Wall Composition in Maturing Tillers of Switchgrass (*Panicum virgatum* L.)." *Bioresource Technology* 98: 2985–2992. <https://doi.org/10.1016/j.biortech.2006.10.020>.
- Sheng, J., X. Zheng, J. Wang, et al. 2017. "Transcriptomics and Proteomics Reveal Genetic and Biological Basis of Superior Biomass Crop Miscanthus." *Scientific Reports* 7: 1–13. <https://doi.org/10.1038/s41598-017-14151-z>.
- Shepherd, A., J. Clifton-Brown, J. Kam, S. Buckby, and A. Hastings. 2020. "Commercial Experience With Miscanthus Crops: Establishment, Yields and Environmental Observations." *GCB Bioenergy* 12: 510–523. <https://doi.org/10.1111/gcbb.12690>.
- Taherzadeh, M. J., and K. Karimi. 2008. "Pretreatment of Lignocellulosic Wastes to Improve Ethanol and Biogas Production: A Review." *International Journal of Molecular Sciences* 9: 1621–1651. <https://doi.org/10.3390/ijms9091621>.
- van der Crujisen, K., M. Al Hassan, G. van Erven, O. Dolstra, and L. M. Trindade. 2021. "Breeding Targets to Improve Biomass Quality in Miscanthus." *Molecules* 26: 1–28. <https://doi.org/10.3390/molecules26020254>.
- van der Crujisen, K., M. Al Hassan, G. van Erven, et al. 2024. "Salt Stress Alters the Cell Wall Components and Structure in *Miscanthus sinensis* Stems." *Physiologia Plantarum* 176: e14430. <https://doi.org/10.1111/ppl.14430>.
- van der Weijde, T., C. L. Alvim Kamei, A. F. Torres, et al. 2013. "The Potential of C4 Grasses for Cellulosic Biofuel Production." *Frontiers in Plant Science* 4: 1–18. <https://doi.org/10.3389/fpls.2013.00107>.
- van der Weijde, T., O. Dolstra, R. G. F. Visser, and L. M. Trindade. 2017. "Stability of Cell Wall Composition and Saccharification Efficiency in Miscanthus Across Diverse Environments." *Frontiers in Plant Science* 7: 1–14. <https://doi.org/10.3389/fpls.2016.02004>.
- van der Weijde, T., L. M. Huxley, S. Hawkins, et al. 2017. "Impact of Drought Stress on Growth and Quality of Miscanthus for Biofuel Production." *GCB Bioenergy* 9: 770–782. <https://doi.org/10.1111/gcbb.12382>.
- van der Weijde, T., C. L. A. Kamei, E. I. Severing, et al. 2017. "Genetic Complexity of Miscanthus Cell Wall Composition and Biomass Quality for Biofuels." *BMC Genomics* 18: 1–15. <https://doi.org/10.1186/s12864-017-3802-7>.
- van der Weijde, T., A. Kiesel, Y. Iqbal, et al. 2017. "Evaluation of *Miscanthus sinensis* Biomass Quality as Feedstock for Conversion Into Different Bioenergy Products." *GCB Bioenergy* 9: 176–190. <https://doi.org/10.1111/gcbb.12355>.
- van der Weijde, T., A. F. Torres, O. Dolstra, A. Dechesne, R. G. F. Visser, and L. M. Trindade. 2016. "Impact of Different Lignin Fractions on Saccharification Efficiency in Diverse Species of the Bioenergy Crop Miscanthus." *Bioenergy Research* 9: 146–156. <https://doi.org/10.1007/s12155-015-9669-z>.
- Van Soest, P. J., J. B. Robertson, and B. A. Lewis. 1991. "Methods for Dietary Fiber, Neutral Detergent Fiber, and Nonstarch Polysaccharides in Relation to Animal Nutrition." *Journal of Dairy Science* 74: 3583–3597. [https://doi.org/10.3168/jds.S0022-0302\(91\)78551-2](https://doi.org/10.3168/jds.S0022-0302(91)78551-2).
- Wagner, M., A. Mangold, J. Lask, E. Petig, A. Kiesel, and I. Lewandowski. 2019. "Economic and Environmental Performance of Miscanthus Cultivated on Marginal Land for Biogas Production." *GCB Bioenergy* 11: 34–49. <https://doi.org/10.1111/gcbb.12567>.
- Wickham, H. 2016. *ggplot2: Elegant Graphics for Data Analysis*. Springer-Verlag. <https://ggplot2.tidyverse.org>.

- Xie, L., S. L. MacDonald, M. Auffhammer, D. Jaiswal, and P. Berck. 2019. "Environment or Food: Modeling Future Land Use Patterns of Miscanthus for Bioenergy Using Fine Scale Data." *Ecological Economics* 161: 225–236. <https://doi.org/10.1016/j.ecolecon.2019.03.013>.
- Xu, N., W. Zhang, S. Ren, et al. 2012. "Hemicelluloses Negatively Affect Lignocellulose Crystallinity for High Biomass Digestibility Under NaOH and H<sub>2</sub>SO<sub>4</sub> Pretreatments in Miscanthus." *Biotechnology for Biofuels* 5: 1. <https://doi.org/10.1186/1754-6834-5-58>.
- Xue, S., O. Kalinina, and I. Lewandowski. 2015. "Present and Future Options for Miscanthus Propagation and Establishment." *Renewable and Sustainable Energy Reviews* 49: 1233–1246. <https://doi.org/10.1016/j.rser.2015.04.168>.
- Yoshida, M., Y. Liu, S. Uchida, et al. 2008. "Effects of Cellulose Crystallinity, Hemicellulose, and Lignin on the Enzymatic Hydrolysis of *Miscanthus sinensis* to Monosaccharides." *Bioscience, Biotechnology, and Biochemistry* 72: 805–810. <https://doi.org/10.1271/bbb.70689>.
- Yu, X. F., Z. H. Yang, Y. H. Xu, et al. 2023. "Effect of Chromium Stress on Metal Accumulation and Cell Wall Fractions in *Cosmos bipinnatus*." *Chemosphere* 315: 137677. <https://doi.org/10.1016/j.chemosphere.2022.137677>.
- Yuan, X., Y. Wang, P. Ji, P. Wu, J. Sheffield, and J. A. Otkin. 2023. "A Global Transition to Flash Droughts Under Climate Change." *Science* 380: 187–191. <https://doi.org/10.1126/science.abn6301>.
- Zeng, X., J. Sheng, F. Zhu, et al. 2020. "Genetic, Transcriptional, and Regulatory Landscape of Monolignol Biosynthesis Pathway in *Miscanthus* × *Giganteus*." *Biotechnology for Biofuels* 13: 1–15. <https://doi.org/10.1186/s13068-020-01819-4>.
- Zeng, X., J. Sheng, F. Zhu, et al. 2020. "Differential Expression Patterns Reveal the Roles of Cellulose Synthase Genes (CesAs) in Primary and Secondary Cell Wall Biosynthesis in *Miscanthus* × *Giganteus*." *Industrial Crops and Products* 145: 112129. <https://doi.org/10.1016/j.indcrop.2020.112129>.
- Zeng, Z., W. Wu, J. Peñuelas, et al. 2023. "Increased Risk of Flash Droughts With Raised Concurrent Hot and Dry Extremes Under Global Warming." *NPJ Climate and Atmospheric Science* 6: 134. <https://doi.org/10.1038/s41612-023-00468-2>.
- Zhai, R., J. Hu, and M. Jin. 2022. "Towards Efficient Enzymatic Saccharification of Pretreated Lignocellulose: Enzyme Inhibition by Lignin-Derived Phenolics and Recent Trends in Mitigation Strategies." *Biotechnology Advances* 61: 108044. <https://doi.org/10.1016/j.biotechadv.2022.108044>.
- Zhang, B., Y. Gao, L. Zhang, and Y. Zhou. 2021. "The Plant Cell Wall: Biosynthesis, Construction, and Functions." *Journal of Integrative Plant Biology* 63: 251–272. <https://doi.org/10.1111/jipb.13055>.
- Zhang, W., Z. Yi, J. Huang, et al. 2013. "Three Lignocellulose Features That Distinctively Affect Biomass Enzymatic Digestibility Under NaOH and H<sub>2</sub>SO<sub>4</sub> Pretreatments in *Miscanthus*." *Bioresource Technology* 130: 30–37. <https://doi.org/10.1016/j.biortech.2012.12.029>.
- Zhong, R., D. Cui, and Z. H. Ye. 2019. "Secondary Cell Wall Biosynthesis." *New Phytologist* 221: 1703–1723. <https://doi.org/10.1111/nph.15537>.
- Zub, H. W., S. Arnoult, and M. Brancourt-Hulmel. 2011. "Key Traits for Biomass Production Identified in Different *Miscanthus* Species at Two Harvest Dates." *Biomass and Bioenergy* 35: 637–651. <https://doi.org/10.1016/j.biombioe.2010.10.020>.

### Supporting Information

Additional supporting information can be found online in the Supporting Information section.